Published in final edited form as:
J Biol Rhythms. 2010 April ; 25(2): 92–102. doi:10.1177/0748730409360963.

Clock Gene Expression during Chronic Inflammation Induced by Infection with *Trypanosoma brucei brucei* in Rats

Gabriella B. S. Lundkvist[*,1], **Michael T. Sellix**[†], **Mikael Nygård**[‡], **Erin Davis**[†], **Marty Straume**[§], **Krister Kristensson**[‡], and **Gene D. Block**[‖]

[*]Swedish Medical Nanoscience Center, Department of Neuroscience, Karolinska Institutet, Stockholm, Sweden

[†]Department of Biology, University of Virginia, Charlottesville, VA

[‡]Department of Neuroscience, Karolinska Institutet, Stockholm, Sweden

[§]Customized Online Biomathematical Research Applications (COBRA), Charlottesville, VA

[‖]Department of Psychiatry and Biobehavioral Science, University of California, Los Angeles, Los Angeles, CA

Abstract

African sleeping sickness is characterized by alterations in rhythmic functions. It is not known if the disease affects the expression of clock genes, which are the molecular basis for rhythm generation. We used a chronic rat model of experimental sleeping sickness, caused by the extracellular parasite *Trypanosoma brucei brucei (Tb brucei)*, to study the effects on clock gene expression. In tissue explants of pituitary glands from *Period1-luciferase* (*Per1-luc*) transgenic rats infected with *Tb brucei*, the period of *Per1-luc* expression was significantly shorter. In explants containing the suprachiasmatic nuclei (SCN), the *Per1-luc* rhythms were flat in 21% of the tissues. We also examined the relative expression of *Per1*, *Clock*, and *Bmal1* mRNA in the SCN, pineal gland, and spleen from control and infected rats using qPCR. Both *Clock* and *Bmal1* mRNA expression was reduced in the pineal gland and spleen following *Tb brucei* infection. Infected rats were periodic both in core body temperature and in locomotor activity; however, early after infection, we observed a significant decline in the amplitude of the locomotor activity rhythm. In addition, both activity and body temperature rhythms exhibited decreased regularity and "robustness." In conclusion, although experimental trypanosome infection has previously been shown to cause functional disturbances in SCN neurons, only 21% of the SCN explants had disturbed *Per1-luc* rhythms. However, our data show that the infection overall alters molecular clock function in peripheral clocks including the pituitary gland, pineal gland, and spleen.

Keywords

clock gene; sleeping sickness; trypanosome; suprachiasmatic nucleus; circadian rhythm; locomotor; body temperature

[1] To whom all correspondence should be addressed: Department of Neuroscience, Karolinska Institutet, Retzius vag 8, SE-17177 Stockholm, Sweden; Gabriella.Lundkvist@ki.se..

Supplementary material for this article is available on the *Journal of Biological Rhythms* Web site at http://jbr.sagepub.com/supplemental.

Human African trypanosomiasis (HAT), also called "sleeping sickness," is an infectious disease caused by subspecies of an extracellular parasite, *Trypanosoma brucei (Tb)*. The disease is associated with an inflammatory condition in which the afflicted patients show no hypersomnia but progressively develop a fragmentation of the circadian sleep-wake cycle (Buguet et al., 1993; Buguet et al., 1989; Schwartz and Escande, 1970), as well as disturbances in the diurnal plasma levels of cortisol, prolactin, and plasma renin, linked to the changes in the internal sleep structure (Brandenberger et al., 1996). Similarly, sleep episodes become fragmented in rat models of the disease using the rodent pathogenic subspecies *Tb brucei* (Grassi-Zucconi et al., 1995; Montmayeur and Buguet, 1994). In such models, certain alterations in the SCN have been found, for example, altered expression of Fos protein (Peng et al., 1994), reduced glutamate receptor expression, and altered rhythmic impulse activity as well as decreased excitatory postsynaptic activity (Lundkvist et al., 1998; Lundkvist et al., 2002). However, it is not clear whether these changes reflect an alteration of intrinsic SCN pacemaker function. To address this question, we employed an in vivo rat model of experimental sleeping sickness to study the impact of this inflammatory condition on clock gene function. To determine if the intrinsic clock mechanism is disturbed in the SCN, and/or in peripheral oscillators such as the pituitary gland, we monitored real-time gene expression of the clock gene *Period (Per) 1* in SCN and pituitary gland tissue explants from *Period1-luciferase (Per1-luc)* transgenic rats infected with *Tb brucei*. We also examined clock gene expression in the pineal gland, one site of early parasite localization, and in the spleen, because it is markedly affected early during infection. In addition, we performed continuous recordings of circadian locomotor activity and body temperature fluctuations to characterize circadian output parameters following infection.

MATERIALS AND METHODS

Animals and Infection Procedure

Male *Per1-luc* transgenic Wistar rats, in which luciferase activity reports transcription of *Per1* (originally developed by H. Tei [Yamazaki et al., 2000]), from the UVa breeding colony were used for bioluminescence recordings. Both male transgenic *Per1-luc* and nontransgenic (wild-type) Wistar rats were used for real-time PCR analyses. Rats were placed in a 12:12-hour light:dark (LD) cycle or constant darkness (DD) and had continuous access to food and water. The rats, 5 to 8 weeks old, were infected by intraperitoneal injections with pleomorphic *Tb brucei* (AnTat 1/1, derived from stabilate EATRO 1125; Laboratory of Serology, Institute of Tropical Medicine "Prince Leopold," Antwerp, Belgium), a subspecies not pathogenic to humans, or injected with vehicle (PSG, phosphate buffered glucose saline; 44 mM NaCl, 60 mM $NaH_2PO_4 \times H_2O$, 83 mM D-glucose; pH 8). Infected rats were always matched against vehicle-injected control rats of the same age. A volume of 0.5 mL containing 25,000 to 30,000 parasites was injected in each animal. After 10 days, parasitemia was verified in blood samples, obtained from tail snips, in a light microscope (20× magnification). Body weight was measured once a week from the time of infection in the LD animals. Molecular analyses were performed 42 days postinfection when the animals were euthanized with a halothane overdose. For long-term recording of activity and body temperature, the rats were monitored until they showed severe signs of disease (defined as severe lethargy, inactivity, lack of exploring, and no food or water intake). At this point, they were euthanized with halothane overdose.

Tissue Culture and Bioluminescence Recordings

Forty-two days postinfection, uninfected control and infected rats were euthanized with CO_2. The brain and pituitary glands were quickly removed. The SCN and pituitary tissues were dissected and cultured on membranes (see Supplementary Online Material; SOM). The cultures were placed within a light-tight incubator holding a constant temperature of 36 °C, and bioluminescence was recorded continuously with Photomultiplier tube (PMT) detector

assemblies (Hamamatsu USA, Bridgewater, NJ). The PMT modules were interfaced to a task-dedicated computer for data acquisition (software written by Tom Breeden, University of Virginia). The PMTs were positioned 1 to 2 cm above the culture dishes. Photon counts were integrated over 1-minute intervals. One group of SCN slices was obtained from the infected and control animals that were housed with running wheels and placed into DD as described above. A second group of control and infected animals was maintained under a 12:12 LD cycle in cages without running wheels. Bioluminescence traces were detrended by baseline subtraction of a 24-hour moving average and then smoothed with a 2-hour running average. Detrended and smoothed data were analyzed for period with a χ^2 periodogram (Lumicycle Analysis software; Actimetrics Inc., Evanston, IL). Chi-square tests for the period of *Per1-luc* expression were considered significant at $p < 0.001$. Period values were compared as a function of treatment with an unpaired Student *t*-test. All comparisons were considered significant at $p < 0.05$. For amplitude analysis, see SOM.

Real-Time PCR

Per1-luc transgenic or wild-type Wistar rats were injected with *Tb brucei* stabilate or vehicle. At day 42 postinfection, total RNA was extracted from tissue samples (SCN, pineal, and spleen) using RNAqueous-4 PCR kit (Ambion, Austin, TX) or the RNeasy Micro kit (Qiagen, Hilden, Germany), following the manufacturer's instructions, except 100 μL lysis/binding solution was used with the RNAqueous-4 kit (Ambion). Briefly, samples were homogenized, bound to filter, washed, and eluted into H_2O. All RNA was treated with DNase I to remove genomic DNA. Spleen total RNA samples were quantified using an Ultrospec 3000 UV/Visible spectrophotometer (Pharmacia Biotech, Uppsala, Sweden). RNA was stored at −80 °C until cDNA synthesis. The iScript cDNA synthesis kit (Bio-Rad, Hercules, CA) was used for cDNA synthesis according to the manufacturer's directions, using a GeneAmp PCR System 9700 thermocycler (Applied Biosystems Inc., Foster City, CA).

For spleen samples, quantitative real-time PCR was performed on the MyiQ real-time PCR detection system (Bio-Rad) using iQ SYBR Green Supermix (Bio-Rad), and data were analyzed using the MyiQ software (Bio-Rad). For SCN and pineal samples, an ABI Prism 7000 sequence detection system (Applied Biosystems) was used with 1× QuantiTect SYBR Green PCR Master Mix (Invitrogen, Carlsbad, CA). There was 0.5 to 1 μL cDNA that was used in a total volume of 25 μL per reaction, and all analyses were performed in triplicate. For primers, see SOM. For the spleen, 2 samples were used from each animal that were averaged to obtain a single value per animal. Data were normalized to the levels of RNA encoding *cyclophilin*, and relative differences were calculated using the $2^{\times\Delta\Delta C_T}$ method (Livak and Schmittgen, 2001). All values of expression levels were calculated relative to values of control mice at ZT 7. Two-way analysis of variance (ANOVA) was performed to determine the main effects of time of day and infection on mRNA expression levels. In all analyses, a significance level of $p < 0.05$ was considered statistically significant.

Wheel-Running Activity Recordings

Transgenic rats were placed in individual cages with running wheels in a 12:12-hour LD cycle. Wheel activity was monitored with ClockLab (Actimetrics Inc.). After 3 to 4 days, rats were infected with *Tb brucei* or injected with vehicle. One group of rats was released into constant darkness (DD). Continuous activity recordings were performed until the rats showed severe signs of disease and were euthanized with halothane overdose.

Cage Activity and Body Temperature Recordings

Transgenic rats were anesthetized with halothane, and a transmitter (Mini Mitter, Bend, OR) was quickly implanted into the peritoneal cavity. The rats were placed in individual cages in a 12:12-hour LD cycle. General locomotor activity and body temperature were monitored using

the Dataquest system (Data Sciences International, St. Paul, MN). Two weeks later, the rats were injected with *Tb brucei* or vehicle and released into DD. Continuous recordings were performed until the rats showed severe signs of disease and were euthanized with halothane overdose.

Statistical Analyses of Activity and Temperature

Two statistical methods were used to analyze wheel running, cage activity, and body temperature data (Pincus, 1991,1992,1994). The first method employed is the fast Fourier transform-nonlinear least squares (FFT-NLLS) as previously described. Briefly, time series were linear-regression detrended by FFT-NLLS to produce zero-mean, zero-slope data. An FFT power spectrum was first calculated. The period, phase, and amplitude of the most powerful spectral peak were used to initialize a 1-component cosine function, which was NLLS minimized to the detrended time series. The statistical significance of each derived rhythmic component was assessed by way of the relative amplitude error (RAE; ratio of amplitude error to most probable amplitude). Theoretically, this metric ranges from 0.0 to 1.0, with 0.0 indicating a rhythm known to infinite precision (zero error) and 1.0 indicating a rhythm that was not statistically significant (error exceeds most probable value). Intermediate values were indicative of varying degrees of rhythmic determination.

The second method used for analysis of rhythmic parameters was the COSOPT algorithm. COSOPT imports data and calculates the mean value and its corresponding standard deviation (SD). Arithmetic linear regressions detrend of the original time series was not performed. Variable weighing of individual time points (by SEMs from replicate measures) was accommodated during analysis for the presence of rhythms at periods between 18 and 30 hours.

Circadian period and $\text{phase}_{\text{max}}$ (time of maximal activity/temperature) were assessed. An additional number of parameters were analyzed as detailed below: Significant circadian spectral power describes the relative amount of circadian versus noncircadian rhythmic patterning. Calculations were performed using the algorithm MC-FFT. A Fourier spectral assessment was performed on data that were performed on data zero padded to at least 2 times the original data series length. Empirical resampling was employed to evaluate statistical significance at 95% probability. One thousand temporally shuffled, randomized surrogates of each original time series were analyzed to produce 1000 corresponding surrogate Fourier spectra from which the mean power and SD were calculated. The fractions of significant spectral power in the 18- to 30-hour period range were then determined. Alpha is a measure of the relative duration active (0 = no activity, and 1 = no rest). For temperature data, it is the relative duration during which the temperature remained above the local mean temperature. ApEn (approximate entropy) is a measure of temporal patterning irregularity, the larger the value the greater irregularity. ApEn calculation is based on quantification of regularity to statistically discriminate time series. ApEn ratio is a relative measure of “maximally” random temporal patterning (0 = completely ordered condition, 1 = maximal randomness). ApEn *Z* scores represent the number of standard deviations that the observed temporal patterning differs from the maximally random condition. Statistical comparisons between experimental groups were made using the Student *t*-test with Welsh correction.

RESULTS

Experimental Infection with *Trypanosoma brucei brucei*

Parasitemia was confirmed in blood sampled from all infected rats at day 10 postinfection (Supplementary Fig. S1). The rats did not show any weight loss or any other signs of disease during the first 4 weeks of infection. Weight loss, or no further weight gain, was observed in some cases starting from the 5th week (5th body weight measurement) postinfection (data not

shown). Rapid and significant weight loss was considered as severe signs of disease, and the animal was at this point euthanized.

The typical course of disease was 31 to 61 days long as in previous studies (Lundkvist et al., 1998; Lundkvist et al., 2002). Of all rats used in the entire study, 1 rat showed severe signs of disease 31 days postinfection, 3 rats showed severe signs of disease at 35 days postinfection, and 2 rats suddenly died 5 weeks postinfection without any previous weight loss or other signs of disease. The rest were euthanized, either 42 days postinfection or later during behavioral analyses when severe signs of disease appeared.

Circadian Rhythms of Clock Gene Expression in SCN Are Not Affected by Trypanosome Infection, but Clock Gene Expressions in Pituitary Gland, Pineal Gland, and Spleen Are Differentially Altered

To investigate if the molecular clock was affected by the infection, we studied clock gene expression by monitoring continuous *Per1-luc* expression in tissue explant cultures and real-time PCR analyses of tissues sampled from infected rats maintained in a 12:12-hour LD cycle. In addition, SCN tissues were also sampled from animals maintained in DD.

Tissues from animals in LD—Trypanosome infection is associated with disturbed endocrine function (Brandenberger et al., 1996; Radomski et al., 1994; Radomski et al., 1995). Consequently, we sampled SCN and pituitary gland tissue from animals maintained in a 12:12-hour LD cycle without wheels (8 infected, 4 controls). Five of 8 infected SCNs, and 3 of 4 controls, were rhythmic (Fig. 1A). Amplitudes and periods were not affected by *Tb brucei* infection in these explants (period in infected: 23.57 ± 0.86 hours v. period in controls: 23.89 ± 0.39 hours; $p > 0.05$, $F = 8.16$). However, *Per1* rhythms in 3 of the SCN explants from infected animals were arrythmic (Fig. 1B). We observed robust circadian rhythms of *Per1-luc* expression in pituitary explants from 7 of the 8 infected rats. The period of *Per1-luc* expression in the pituitary gland was significantly shorter in tissue from infected rats (21.97 ± 0.18 hours) when compared with uninfected controls (4 rats, 22.63 ± 0.14 hours; $p < 0.05$, $F = 2.86$) (Fig. 1C). The pituitary amplitude was not significantly altered (data not shown).

SCN tissues from animals in DD—We sampled SCN tissue from the same animals that were used for wheel-running analysis in DD (6 infected, 4 controls). All the sampled SCN tissues from DD animals were rhythmic. As with SCNs from LD animals, we did not observe an effect of infection on the average amplitude (data not shown) or period of *Per1-luc* expression in the SCN (infected SCN: 24.56 ± 20 hours v. control SCN: 25.12 ± 0.53 hours; $p > 0.05$, $F = 10.74$).

***Real-time PCR analysis of* Per1, Clock, *and* Bmal1—**To confirm results obtained from in vitro luminescence recordings and examine clock gene expression in the trypanosome-invaded pineal gland and the trypanosome-activated spleen, we performed qPCR analyses on SCN, pineal gland, and spleen sampled at 2 time points from infected (6 rats at ZT 7; 5 rats at ZT 19; 42 days postinfection) and control rats (4 rats at ZT 7; 4 rats at ZT 19) maintained in a 12:12-hour LD cycle without running wheels. RNA was extracted, and the amounts of *Per1*, *Clock*, and *Bmal1* were determined with real-time PCR. In the SCN, we did not observe a significant difference in the patterns of *Per1*, *Clock*, or *Bmal1* expression between controls and infected animals. In both groups, *Per1* showed diurnal differences (data not shown) with increased amounts during the day ($p < 0.0001$; 2-way ANOVA), thus confirming the in vitro data obtained from *Per1-luc* recordings. *Bmal1* also showed diurnal differences in both groups, with higher expression at ZT 19 ($p < 0.02$; 2-way ANOVA), whereas *Clock* did not show significant diurnal differences (data not shown).

In the pineal gland, *Per1* and *Bmal1* showed diurnal differences (expression in antiphase as compared to the SCN) in both control and infected animals ($p < 0.0001$, $p = 0.002$; 2-way ANOVA). *Clock* showed no significant diurnal differences in control and infected animals; however, the total amount of *Clock* was significantly reduced in pineal glands from infected animals ($p = 0.0002$; 2-way ANOVA) (Fig. 2A).

We did not detect a significant diurnal rhythm of *Per1*, *Clock*, or *Bmal1* mRNA expression in the spleen from either control or infected rats. However, *Bmal1* expression was significantly reduced in spleens from infected animals ($p = 0.03$; 2-way ANOVA) (Fig. 2B).

Light-Entrained and Free-Running Circadian Rhythms of Locomotor Activity Are Weakened by Trypanosome Infection

We next examined wheel-running behavior of rats infected with trypanosomes and maintained in a 12:12-hour LD cycle or in DD. Control rats (LD, $n = 4$; DD, $n = 5$) and trypanosome-infected rats (LD, $n = 7$; DD, $n = 6$) showed rhythmicity in wheel-running activity both in LD (Fig. 3A, B) and DD (Fig. 4A, B). One of the infected rats in LD, however, became behaviorally arrhythmic at the end of the infection course (Fig. 3C).

Infected rats produced less spectral power in the circadian range in both LD ($p = 0.044$) and DD ($p = 0.05$) relative to controls. The regularity of the locomotor activity rhythm was significantly decreased ($p = 0.008$) as detected by FFT-NLLS SD-RAE. Infected and control rats exhibited either no significant difference in period lengths (COSOPT $p = 0.2250$) or a significant period difference in LD (FFT-NLLS $p = 0.029$; period in infected group was longer), depending on the statistical analysis employed (Table 1). See Table 1 for the exact values of all different parameters.

Statistical tests confirmed no significant difference between LD and DD rhythms of activity (comparisons between LD and DD are not shown in table) for each parameter with the exception of FFT-NLLS SD-RAE in the infected group, which was significantly higher (rhythm is “less determined” or “less regular”) in LD than in DD ($p = 0.019$).

Circadian Rhythms of General Cage Activity and Body Temperature Are Weakened by Trypanosome Infection

To perform continuous recordings of body temperature, and to rule out the possibility that the excessive amount of physical activity associated with wheel-running activity might conceal subtle behavioral effects of infection, we implanted transponders into the peritoneal cavities of adult rats and infected them with *Tb brucei*. The transponders monitored locomotor activity and body temperature.

Cage activity—As for wheel-running activity, the cage activity was rhythmic but significantly “weaker.” As described in Table 2 and indicated by the representative activity record in Supplementary Figure S2, compared to controls ($n = 4$), the trypanosome-infected rats ($n = 6$) showed significantly lower amplitudes of the cage activity rhythms ($p = 0.0122$, COSOPT), but the average period of trypanosome-infected rats did not significantly differ from controls. The activity rhythms from infected rats were significantly reduced in regularity and less “determined” than controls ($p = 0.0007$; as measured by RAE) (Table 2). No difference in circadian spectral power was found between control animals and infected animals.

Body temperature rhythms—Control rats ($n = 4$) and trypanosome-infected rats ($n = 6$) showed clear rhythms in core body temperature; however, the rhythms from infected rats were significantly reduced in regularity and less “determined” than controls (as measured by RAE; $p = 0.004$) (Fig. 4 and Table 3). These “sloppy” body temperature rhythms were more apparent

during the second half of the infection course (Fig. 4F). In the 2 transponder animals (out of 6 infected) that survived longer than 50 days, the rhythms were difficult to distinguish in the body temperature records. The periods and amplitudes of the temperature rhythms did not significantly differ between the 2 groups. The mean overall body temperatures did not differ significantly between controls (37.9 °C ± 0.248 °C) and trypanosome-infected rats (37.7 °C ± 0.255 °C).

Cross-correlation (CC) analysis demonstrated positive correlations between cage activity patterning and body temperature rhythms in both control (CC = 0.770 ± 0.016; *Z* score = 33.8 ± 0.8) and infected (CC = 0.591 ± 0.020; *Z* score = 17.2 ± 2.0) rats. These correlations were stronger in control than in infected animals ($p = 0.0002$ and $p = 0.0003$ for CC and *Z* score, respectively).

DISCUSSION

Does Experimental Sleeping Sickness Affect Circadian Rhythms of Clock Gene Expression in Central and/or Peripheral Oscillators?

We found that circadian oscillation of *Per1-luc* expression in the majority of SCN explants does not appear to be affected by experimental sleeping sickness. However, 3 of the total 14 infected animals failed to show a rhythm of *Per1-luc* expression in the SCN. The reason for this is not clear; however, because there is a large interindividual heterogeneity in survival time and the immune response to the trypanosome infection, we speculate that *Per1* rhythmicity in the SCN function can be affected in certain individuals. The differential effect of trypanosome infection on SCN clock gene expression can be due to the extent of brain invasion by the parasites. The SCN is protected by the blood-brain barrier (BBB), whereas the pineal and pituitary glands, on the other hand, are located outside the BBB and are infiltrated early by parasites (Schultzberg et al., 1988). The pituitary gland exhibited a significant shortening of the *Per1-luc* period in infected tissues. This is of interest because trypanosome infection causes disturbed rhythmic secretion of cortisol and prolactin (Brandenberger et al., 1996), and hypothalamic neuroendocrine control of both prolactin and corticosterone (cortisol) secretions is regulated by a hierarchy of circadian clocks in the SCN, arcuate nucleus, and pituitary gland (Freeman et al., 2000; Leclerc and Boockfor, 2005; Palm et al., 2001; Sellix et al., 2006). Our data suggest that trypanosome infection affects the hypothalamicpituitary axis, and altered clock function within pituitary cells may contribute to the altered hormone secretory profiles associated with trypanosome infection. In addition, we found a significantly reduced amount of *Clock* mRNA in the melatoninproducing pineal gland, indicating an alteration in rhythmic pineal function. Interestingly, it has been found that the sleep-wake pattern was restored by melatonin administration in rats infected with trypanosomes (Grassi-Zucconi et al., 1996). Finally, our real-time PCR analysis revealed a significantly reduced expression of *Bmal1* mRNA in the spleen of infected rats. The spleen is strongly affected and enlarged in trypanosome-infected animals, which led us to believe that clock gene activity in the immunoactivated splenocytes may be altered by trypanosome infection. Taken together, our clock gene analyses suggest that peripheral oscillators outside the BBB are generally impacted by trypanosome infection. We speculate that disturbed endocrine signals from the affected pineal and pituitary glands could influence rhythms of locomotor and temperature activity, perhaps via feedback signaling to the SCN. As reviewed by Buijs et al. (2006), it has been suggested that endocrine and metabolic signals can indeed affect the SCN.

In a previous study, we observed that electrical properties of SCN neurons in brain slices are altered by trypanosome infection. The characteristic daily increase in spontaneous impulse activity was decreased, and the “peak” of activity normally observed around ZT 6 to 7 was advanced by almost 3 hours (Lundkvist et al., 1998). Furthermore, the frequency of spontaneous excitatory postsynaptic events was decreased in acute SCN slices sampled from

infected rats (Lundkvist et al., 2002), indicating a presynaptic effect possibly as a result of the decreased impulse activity during the subjective day. Because we found clock gene alterations in only 21% of the infected SCN explants, the altered electrical function in trypanosome-infected SCN neurons may not be associated with changes in the functioning of the molecular clock but rather by alterations at the level of membrane events.

Trypanosome-Infected Rats Show Activity and Temperature Rhythms that Are Significantly Weakened

Overall, we found that our infected rats have normal average body temperature and show circadian rhythms of locomotor activity, which can be entrained by the environmental LD cycle and free run in DD. The only exception was one infected rat in LD that became arrhythmic at the end of the running record (Fig. 3C). However, the activity records showed alterations of several rhythmic parameters. The period was longer in LD-infected rats, and marked reductions in amplitude, robustness, and power of the 24-hour activity rhythms were overall observed. Our data confirm and extend an earlier study (Grassi-Zucconi et al., 1995) in which reduced locomotor activity during the light phase was reported in trypanosome-infected rats. Further, our transponder analysis of the rhythm in body temperature revealed that the rhythms were sustained but became significantly less robust in infected animals. This was most obvious from days 45 to 50 of the infection course (compare Fig. 5E and 5F). Our results are similar to the data presented in the study by Chevrier et al. (2005) in which deteriorations of body temperature and activity rhythms were observed at the end of the *Tb brucei* infection course in Sprague Dawley rats, accompanied by abrupt alterations in body weight and food intake. One difference between the studies is that in our more chronic infection model, the activity rhythm amplitude was significantly reduced already at the beginning after infection with parasites. Nevertheless, the 2 studies both suggest weaker and blunted rhythms in experimental *Tb brucei* rat infection, an effect that appears to be most prominent at the end of the infection course.

Concluding Remarks

Our study demonstrates that sleeping sickness affects clock gene expression but not primarily by altering the molecular processes that underlie rhythm generation in the SCN. However, the use of a highly heterogeneous experimental model that is dependent on the individual animal's immune response prevents us from ruling out the possibility that the infection may also impact clock gene expression in the SCN because 1) we observed flat *Per1-luc* expression in 3 of 14 SCN tissues; 2) one rat showed arrhythmic locomotor activity at the end of infection; and 3) the body temperature rhythms in 2 long-surviving animals containing transponders were almost indistinguishable at the end of infection. Our data reveal that parasitic infection affects the circadian system at levels downstream of the SCN molecular clock by altering molecular oscillations in peripheral oscillators, including the pituitary gland, the pineal gland, and the spleen. These tissues are critically important for homeostatic regulation of the endocrine, immune, and sleep physiology. Thus, the effects of sleeping sickness on the entire circadian system may provide new insights into the etiology of inflammatory conditions associated with decline in the robustness of biological rhythms.

Supplementary Material

Refer to Web version on PubMed Central for supplementary material.

Acknowledgments

This work was supported by Swedish Research Council K2008-61X-20700-01-3 and K2009-75SX-21028-01-3, Jeansson's foundation, Wolff's foundation, and Söderström-Königska foundation to G.B.S.L.; European Union (FP6-2004-INCO-DEV-3 032324; NEUROTRYP) to K.K.; and R01 HL71510 and R01 MH062517-04A1 to G.D.B.

REFERENCES

Brandenberger G, Buguet A, Spiegel K, Stanghellini A, Muanga G, Bogui P, Dumas M. Disruption of endocrine rhythms in sleeping sickness with preserved relationship between hormonal pulsatility and the REM-NREM sleep cycles. J Biol Rhythms 1996;11:258–267. [PubMed: 8872597]

Buguet A, Bert J, Tapie P, Tabaraud F, Doua F, Lonsdorfer J, Bogui P, Dumas M. Sleep-wake cycle in human African trypanosomiasis. J Clin Neurophysiol 1993;10:190–196. [PubMed: 8389383]

Buguet A, Gati R, Sevre JP, Develoux M, Bogui P, Lonsdorfer J. 24 hour polysomnographic evaluation in a patient with sleeping sickness. Electroencephalogr Clin Neurophysiol 1989;72:471–478. [PubMed: 2471615]

Buijs RM, Scheer FA, Kreier F, Yi C, Bos N, Goncharuk VD, Kalsbeek A. Organization of circadian functions: interaction with the body. Prog Brain Res 2006;153:341–360. [PubMed: 16876585]

Chevrier C, Canini F, Darsaud A, Cespuglio R, Buguet A, Bourdon L. Clinical assessment of the entry into neurological state in rat experimental African trypanosomiasis. Acta Trop 2005;95:33–39. [PubMed: 15882835]

Freeman ME, Kanyicska B, Lerant A, Nagy G. Prolactin: structure, function, and regulation of secretion. Physiol Rev 2000;80:1523–1631. [PubMed: 11015620]

Grassi-Zucconi G, Harris JA, Mohammed AH, Ambrosini MV, Kristensson K, Bentivoglio M. Sleep fragmentation, and changes in locomotor activity and body temperature in trypanosome-infected rats. Brain Res Bull 1995;37:123–129. [PubMed: 7606487]

Grassi-Zucconi G, Semprevivo M, Mocaer E, Kristensson K, Bentivoglio M. Melatonin and its new agonist S-20098 restore synchronized sleep fragmented by experimental trypanosome infection in the rat. Brain Res Bull 1996;39:63–68. [PubMed: 8846114]

Leclerc GM, Boockfor FR. Pulses of prolactin promoter activity depend on a noncanonical E-box that can bind the circadian proteins CLOCK and BMAL1. Endocrinology 2005;146:2782–2790. [PubMed: 15774559]

Livak KJ, Schmittgen TD. Analysis of relative gene expression data using real-time quantitative PCR and the 2(-Delta Delta C(T)) method. Methods 2001;25:402–408. [PubMed: 11846609]

Lundkvist GB, Christenson J, ElTayeb RA, Peng ZC, Grillner P, Mhlanga J, Bentivoglio M, Kristensson K. Altered neuronal activity rhythm and glutamate receptor expression in the suprachiasmatic nuclei of Trypanosoma brucei-infected rats. J Neuropathol Exp Neurol 1998;57:21–29. [PubMed: 9600194]

Lundkvist GB, Hill RH, Kristensson K. Disruption of circadian rhythms in synaptic activity of the suprachiasmatic nuclei by African trypanosomes and cytokines. Neurobiol Dis 2002;11:20–27. [PubMed: 12460543]

Montmayeur A, Buguet A. Time-related changes in the sleep-wake cycle of rats infected with Trypanosoma brucei brucei. Neurosci Lett 1994;168:172–174. [PubMed: 7913215]

Palm IF, van der Beek EM, Swarts HJ, van der Vliet J, Wiegant VM, Buijs RM, Kalsbeek A. Control of the estradiol-induced prolactin surge by the suprachiasmatic nucleus. Endocrinology 2001;142:2296–2302. [PubMed: 11356675]

Peng ZC, Kristensson K, Bentivoglio M. Dysregulation of photic induction of Fos-related protein in the biological clock during experimental trypanosomiasis. Neurosci Lett 1994;182:104–106. [PubMed: 7891872]

Pincus SM. Approximate entropy as a measure of system complexity. Proc Natl Acad Sci U S A 1991;88:2297–2301. [PubMed: 11607165]

Pincus SM. Approximating Markov chains. Proc Natl Acad Sci U S A 1992;89:4432–4436. [PubMed: 11607293]

Pincus SM. Quantification of evolution from order to randomness in practical time series analysis. Methods Enzymol 1994;240:68–89. [PubMed: 7823854]

Radomski MW, Buguet A, Bogui P, Doua F, Lonsdorfer A, Tapie P, Dumas M. Disruptions in the secretion of cortisol, prolactin, and certain cytokines in human African trypanosomiasis patients. Bull Soc Pathol Exot 1994;87:376–379. [PubMed: 7496204]

Radomski MW, Buguet A, Montmayeur A, Bogui P, Bourdon L, Doua F, Lonsdorfer A, Tapie P, Dumas M. Twenty-four-hour plasma cortisol and prolactin in human African trypanosomiasis patients and healthy African controls. Am J Trop Med Hyg 1995;52:281–286. [PubMed: 7694972]

Schultzberg M, Ambatsis M, Samuelsson EB, Kristensson K, van Meirvenne N. Spread of Trypanosoma brucei to the nervous system: early attack on circumventricular organs and sensory ganglia. J Neurosci Res 1988;21:56–61. [PubMed: 3216412]

Schwartz BA, Escande C. Sleeping sickness: sleep study of a case. Electroencephalogr Clin Neurophysiol 1970;29:83–87. [PubMed: 4194054]

Sellix MT, Egli M, Poletini MO, McKee DT, Bosworth MD, Fitch CA, Freeman ME. Anatomical and functional characterization of clock gene expression in neuroendocrine dopaminergic neurons. Am J Physiol Regul Integr Comp Physiol 2006;290:R1309–1323. [PubMed: 16373438]

Yamazaki S, Numano R, Abe M, Hida A, Takahashi R, Ueda M, Block GD, Sakaki Y, Menaker M, Tei H. Resetting central and peripheral circadian oscillators in transgenic rats. Science 2000;288:682–685. [PubMed: 10784453]

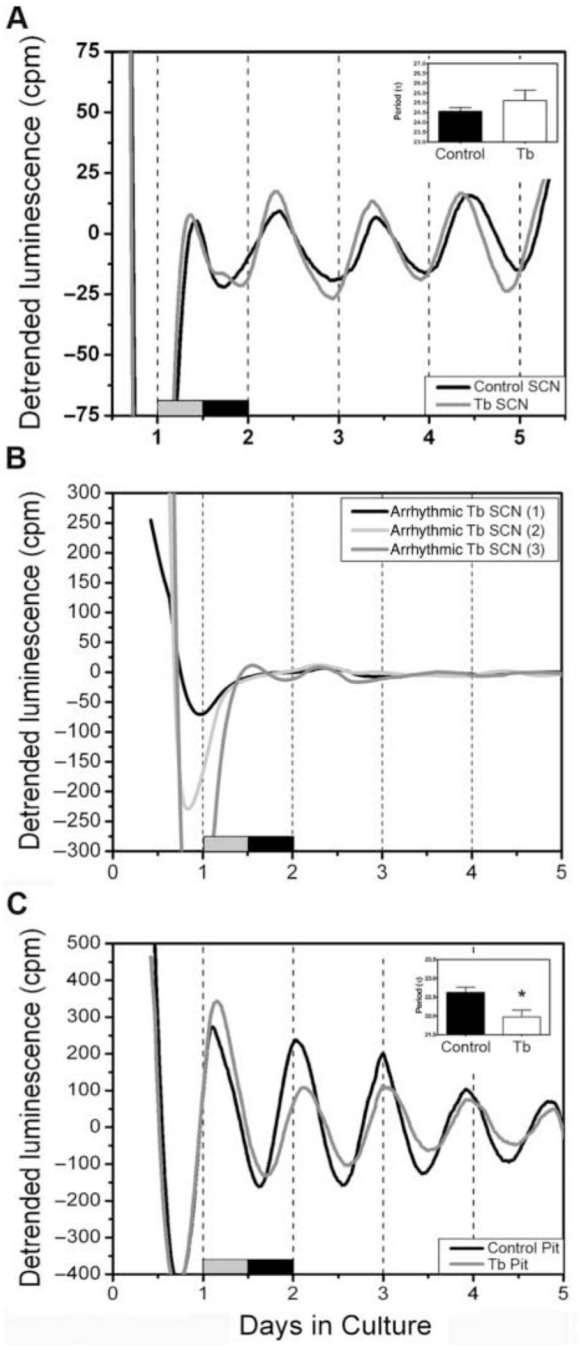

Figure 1.

Effects of *Tb brucei* infection on the circadian rhythms of *Per1-luc* expression. (A) Representative *Per1-luc* expression rhythms in isolated SCN tissue explants recovered from control (black trace) or *Tb brucei*–infected (gray trace) rats in 12:12-hour LD. (B) In 3 of the SCN explants, rhythms were blunted and/or absent. (C) Representative *Per1-luc* expression rhythms in isolated pituitary tissue explants recovered from control (black trace) or *Tb brucei* (gray trace). The period (insert) of *Per1-luc* expression in pituitary glands from animals maintained in LD was significantly shorter in *Tb brucei* infection, indicated by the asterisk. The gray-black bars at the bottom of the figures indicate the LD cycle prior to sacrifice.

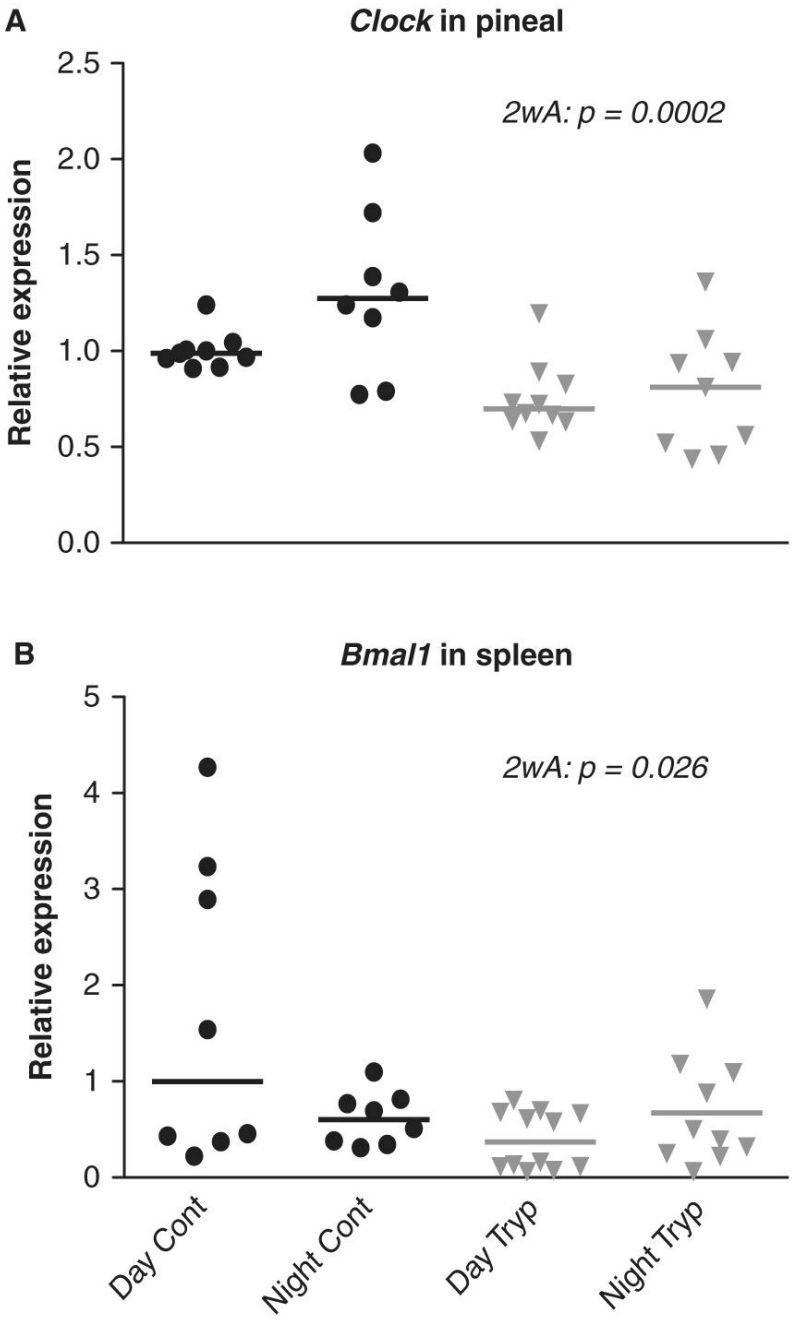

Figure 2.
Relative amounts of (A) *Clock* in the pineal gland and (B) *Bmal1* in spleen sampled from control and infected rats at ZT 6 to 7 (Day cont; tryp) and ZT 18 to 19 (Night cont; tryp). Two-way ANOVA (2wA) showed significant differences between control and infected groups.

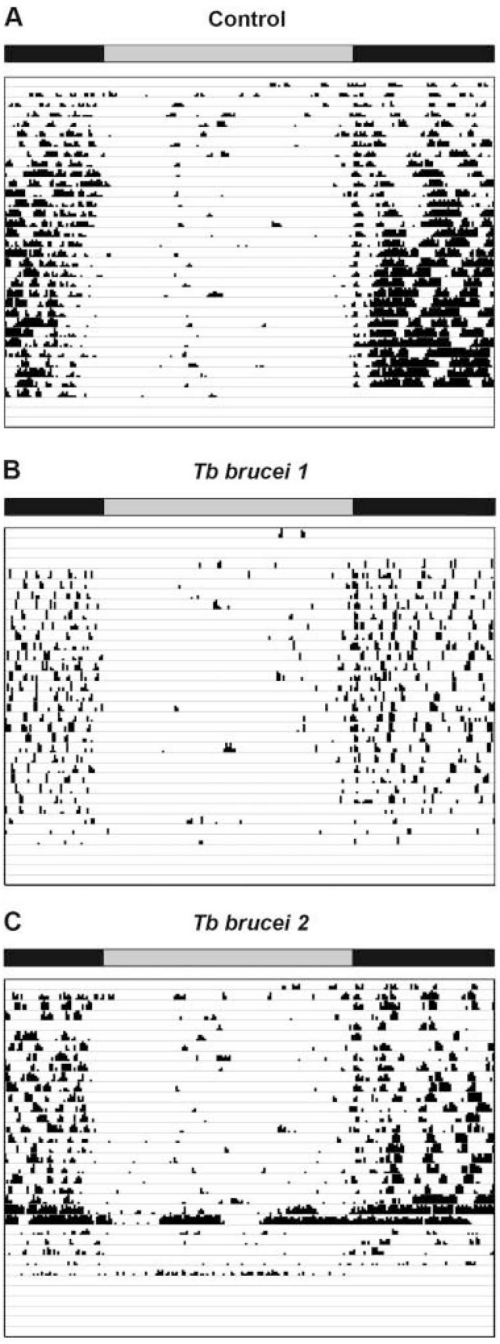

Figure 3.
Example of actograms obtained from wheel-running activity in a 12:12-hour light:dark cycle from 1 control rat and 2 rats infected with *Tb brucei*, respectively. The record from the first infected rat ("*Tb brucei* 1") is representative for the infected group; however, the second record shown ("*Tb brucei* 2") demonstrates arrhythmicity in one infected rat at the end of the activity recording period. The top horizontal bar indicates the time of subjective night (black) and day (gray).

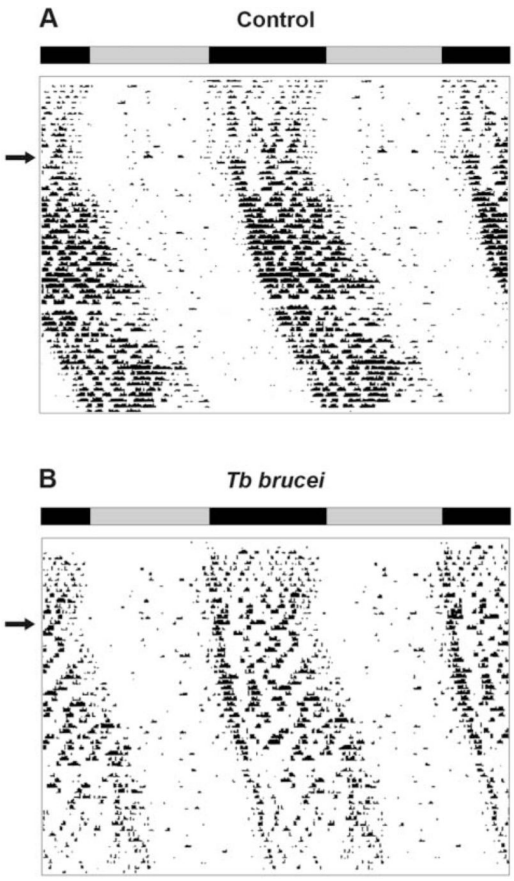

Figure 4.
Example of double-plotted actograms obtained from wheel-running activity in constant darkness from (A) 1 control and (B) 1 infected rat, respectively. The rats were first held in a 12:12-hour LD cycle, indicated by the bars, before released into constant darkness (arrows).

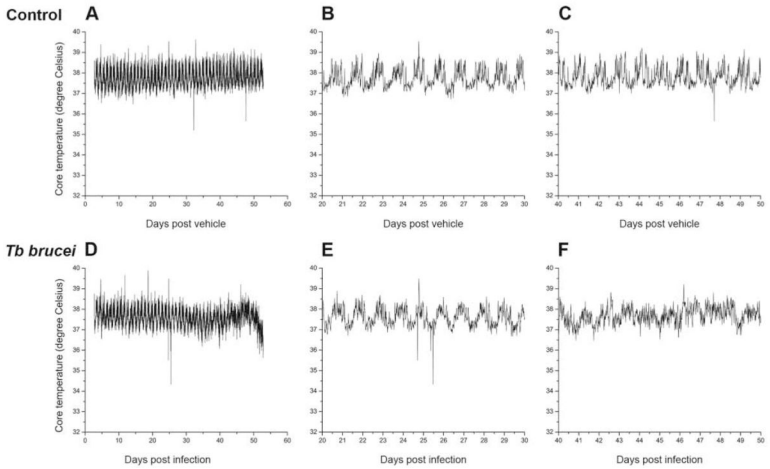

Figure 5.
Core body temperature records from 1 control (A-C) and 1 infected (D-F) rat. B and E show magnifications of postinfection days 20 to 30, and C and F show magnifications of postinfection days 40 to 50.

Table 1

Wheel-running activity in LD and DD.

	LD			DD		
Property	**Control (*n* = 4)**	**Infected (*n* = 7)**	**p**	**Control (*n* = 5)**	**Infected (*n* = 6)**	**p**
MC-FFT	**42.8 ± 5.5**	**23.6 ± 1.5**	**0.044**	**37.8 ± 3.0**	**26.9 ± 3.6**	**0.050**
FFT-NLLS period	**23.93 ± 0.02**	**24.01 ± 0.02**	**0.029**	24.01 ± 0.17	23.88 ± 0.10	0.509
COSOPT period	23.95 ± 0.03	24.01 ± 0.03	0.225	24.06 ± 0.15	24.03 ± 0.11	0.873
FFT-NLLS phase (max)	−0.25 ± 0.40	−1.20 ± 0.38	0.142	−1.87 ± 1.90	0.19 ± 1.24	0.373
COSOPT phase (max)	−0.24 ± 0.56	−1.38 ± 0.49	0.177	−2.50 ± 1.68	−1.99 ± 1.27	0.811
FFT-NLLS SD-RAE	**0.095 ± 0.017**	**0.183 ± 0.017**	**0.008**	0.070 ± 0.007	0.108 ± 0.022	0.161
Alpha	**0.174 ± 0.018**	**0.130 ± 0.008**	**0.029**	0.179 ± 0.02	0.160 ± 0.013	0.432
ApEn	1.294 ± 0.069	1.400 ± 0.038	0.173	1.301 ± 0.025	1.378 ± 0.038	0.141
ApEn ratio	0.785 ± 0.042	0.884 ± 0.027	0.077	**0.785 ± 0.018**	**0.853 ± 0.020**	**0.035**
ApEn *Z* scores	−25.1 ± 8.4	−8.3 ± 2.7	0.153	**−35.9 ± 7.7**	**−16.6 ± 3.6**	**0.039**

Bolded numbers indicate statistical significance.

Table 2

Cage activity.

Property	Control (n = 4)	Infected (n = 6)	p
Amplitude	**33.9 ± 3.15**	**13.7 ± 5.32**	**0.012**
MC-FFT	39.2 ± 0.8	39.4 ± 2.9	0.950
FFT-NLLS period	24.51 ± 0.03	24.35 ± 0.07	0.116
COSOPT period	24.50 ± 0.04	24.45 ± 0.06	0.556
FFT-NLLS phase (max)	**−7.38 ± 0.038**	**−5.49 ± 0.53**	**0.031**
COSOPT phase (max)	**−7.11 ± 0.46**	**−5.71 ± 0.39**	**0.050**
FFT-NLLS SD-RAE	**0.137 ± 0.016**	**0.246 ± 0.013**	**0.0007**
Alpha	0.431 ± 0.011	0.405 ± 0.010	0.121
ApEn	**2.167 ± 0.022**	**2.047 ± 0.018**	**0.003**
ApEn ratio	0.981 ± 0.005	0.974 ± 0.007	0.487
ApEn *Z* scores	−5.3 ± 1.3	−3.2 ± 0.7	0.158

Bolded numbers indicate statistical significance.

Table 3

Body temperature.

Property	Control (*n* = 4)	Infected (*n* = 6)	p
Amplitude	0.362 ± 0.018	0.332 ± 0.035	0.533
MC-FFT	60.5 ± 2.0	61.3 ± 2.7	0.835
FFT-NLLS period	24.50 ± 0.04	24.34 ± 0.07	0.124
COSOPT period	24.50 ± 0.04	24.43 ± 0.06	0.415
FFT-NLLS phase (max)	−7.31 ± 0.314	−6.60 ± 0.32	0.169
COSOPT phase (max)	−7.54 ± 0.37	−6.36 ± 0.45	0.099
FFT-NLLS SD-RAE	**0.054 ± 0.006**	**0.090 ± 0.006**	**0.004**
Alpha	**0.429 ± 0.013**	**0.479 ± 0.010**	**0.015**
ApEn	1.950 ± 0.045	1.888 ± 0.042	0.357
ApEn ratio	0.880 ± 0.016	0.880 ± 0.009	1.000
ApEn *Z* scores	**−42.4 ± 5.8**	**−23.5 ± 2.2**	**0.008**

Bolded numbers indicate statistical significance.